

Beta-limiting MHD instabilities in improved performance NSTX spherical torus plasmas

J.E. Menard 1), M.G. Bell 1), R.E. Bell 1), E.D. Fredrickson 1), D.A. Gates 1), S.M. Kaye 1), B.P. LeBlanc 1), R. Maingi 2), D. Mueller 1), S.A. Sabbagh 3), D. Stutman 4), C.E. Bush 2), D.W. Johnson 1), R. Kaita 1), H.W. Kugel 1), R.J. Maqueda 5), F. Paoletti 3), S.F. Paul 1), M. Ono 1), Y.-K.M. Peng 2), C.H. Skinner 1), E.J. Synakowski 1), and the NSTX Research Team.

1) Princeton Plasma Physics Laboratory, Princeton, NJ, USA

2) Oak Ridge National Laboratory, Oak Ridge, TN, USA

3) Columbia University, New York, NY, USA

4) Johns Hopkins University, Baltimore, MD, USA

5) Los Alamos National Laboratory, Los Alamos, NM, USA

email-contact of main author: jmenard@pppl.gov

Abstract. Global magnetohydrodynamic stability limits in the National Spherical Torus Experiment (NSTX) have increased significantly recently due to a combination of device and operational improvements. First, more routine H-mode operation with broadened pressure profiles allows access to higher normalized beta and lower internal inductance. Second, the correction of a poloidal field coil induced error-field has largely eliminated locked tearing modes during normal operation and increased the maximum achievable beta. As a result of these improvements, peak beta values have reached (not simultaneously) $\beta_t = 35\%$, $\beta_N = 6.5$, $\langle\beta_N\rangle = 4.5$, $\beta_N/l_i = 10$, and $\beta_P = 1.4$. High β_P operation with reduced tearing activity has allowed a doubling of discharge pulse-length to just over 1 second with sustained periods of $\beta_N \approx 6$. Details of the β limit scalings and β -limiting instabilities in various operating regimes are described.

1. Introduction

Recent experiments on the National Spherical Torus Experiment (NSTX) [1, 2] have made significant progress in reaching high toroidal beta $\beta_t \leq 35\%$ and in achieving long discharge duration by operating at high poloidal beta $\beta_P \leq 1.4$ in separate operating regimes. Typical parameters for present NSTX plasmas are: major radius $R_0 = 85\text{-}90$ cm, aspect ratio $A=R_0/a > 1.3\text{-}1.5$, elongation $\kappa < 2.4$, triangularity $\delta < 0.8$, vacuum toroidal field $B_{t0} = 0.3\text{-}0.6$ Tesla at R_0 , plasma current $I_P < 1.5$ MA, and plasma pulse length up to 1 second. High temperature bake-out of the plasma facing components has reduced impurity levels and allowed more reliable access to the H-mode. The broader pressure profile and reduced internal inductance resulting from increased off-axis bootstrap current has permitted operation with significantly higher normalized beta $\beta_N \approx 6$. A poloidal field coil induced error field was also discovered and corrected. This correction largely eliminated locked tearing modes during normal operation and effectively raised the β limit by facilitating routine operation above the no-wall limit in regimes with sufficiently high plasma rotation, elevated $q(0)$, and broad pressure profiles. Finally, boundary shape and discharge evolution optimizations have resulted in discharges with extended periods free of both edge localized modes (ELMs) and sawtooth activity. In such regimes, high β_P has

been combined with high β_N to achieve 800kA discharges with sustained operation above the ideal no-wall stability limit for several energy confinement times and many resistive wall times. Tearing modes are found to limit the achievable β at high β_t and to degrade but not severely limit confinement in regimes with high β_P .

2. Error fields and locked modes

In order to investigate locked mode and resistive wall mode (RWM) physics in NSTX, a radial field detector array was installed to measure $n=1$ radial magnetic field perturbations. Six large-area B_R sensors cover the full toroidal extent of NSTX, and the sensors are mounted symmetrically about the mid-plane and very close to the PF5 primary vertical field (VF) coils. Early in the commissioning of these detectors it became apparent that a large effective shift of the lower PF5 coil was generating predominantly $n=1$ error-field over much of the NSTX plasma volume and local error-field magnitudes as large as 50 Gauss near the outboard plasma boundary. For reference, the equilibrium field magnitude at the same location is typically 3-5 kGauss.

Detailed spatial measurements of the coil shape confirmed the magnetic measurements, and the coil was subsequently shifted and re-shaped to minimize the $n=1$ error field component. Measurements of the corrected coil shape indicate that the $n=1$ error field strength has been reduced by an order of magnitude. This reduction led immediately to improved performance - most noticeably in the locking behavior of ohmic discharges and beam-heated H-mode discharges. Figures 1a-c illustrate that prior to error field reduction (dashed curves) ohmic discharges routinely exhibited disruptions in plasma current and density during the I_P flat-top phase. These disruptions typically occurred once the $q=2$ surface entered the plasma and grew to sufficiently large minor radius. Figure 1d shows the typical 15-30ms growth time of a 4 Gauss locked mode which led to disruption. In contrast, the solid curves in Figure 1 show that for very similar discharge parameters there is no locking behavior evident until the solenoid current limit is reached (near $t=290$ ms) and strong negative loop voltage is applied which disrupts the plasma. Prior to error field correction it was often difficult to avoid ohmic locked modes at any density. Subsequent density scans in the reduced error field configuration found locked modes could again be excited if the line-average density fell below $1.8 \times 10^{19} m^{-3}$ at $t=250$ ms. This density is generally exceeded under normal operating

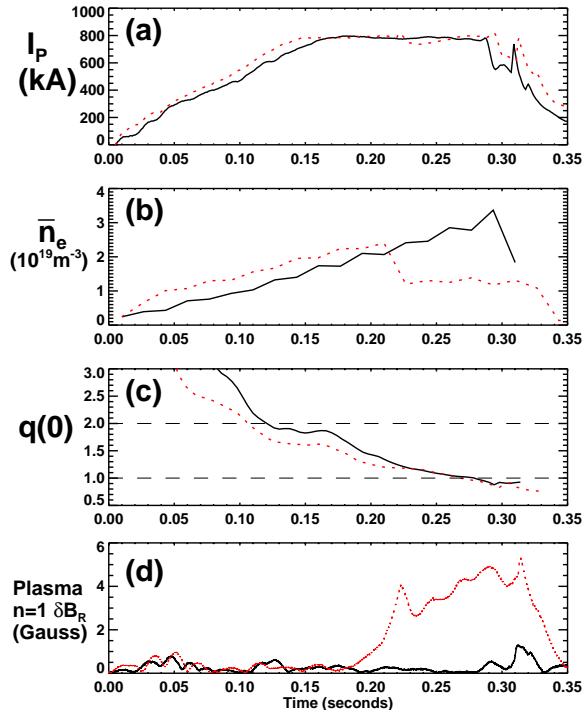


Figure 1: Comparison of $I_P=800kA$, $B_{t0}=4.5kG$ ohmic discharges before (dashed) and after (solid) re-alignment of the primary vertical field (PF5) coils on NSTX. (a) plasma current, (b) line-average density, (c) $q(0)$, and (d) $n=1$ locked mode amplitude measured outside the vessel.

conditions, and no longer limits performance in most circumstances. It should be noted that at the present time, only the shape of the PF5 coil set has been accurately measured, and other coils and current carrying structures may also be generating error fields. Internal toroidal arrays of radial and vertical field sensors placed above and below the midplane are presently being commissioned on NSTX to better diagnose the structure of error fields, locked modes, and resistive wall modes.

3. Global Stability Improvements

In addition to the aforementioned error field reduction, NSTX now has the capability of high-temperature (350°C) bake-out of its graphite plasma facing components. This has led to comparatively easy access to the H-mode [3] and significantly broader pressure profiles, which are predicted to improve stability in various NSTX operating regimes [4, 5]. These improvements are synergistic, as H-mode operation prior to error field reduction was often degraded by the excitation of 2/1 tearing modes [6] which routinely slowed, locked, and disrupted the plasma.

Figure 2 shows the significant increase in β due to these improvements. As seen in the figure, $\beta_N \geq 6$ as determined by EFIT reconstructions [7, 8, 9] has now been achieved for a wide range of normalized currents, and toroidal beta values $\beta_t \equiv 2\mu_0\langle p \rangle / B_{t0}^2$ as high as 35% have been achieved. The limits prior to these improvements are shown by the black symbols on the same figure. Figure 3 plots toroidal β values re-scaled to remove leading geometric terms in the dimensionless form of Sykes-Troyon scaling [10, 11]. As seen in the figure, prior to error field reduction and bake-out $\epsilon\beta_P$ was limited to approximately 0.45. This limit was set primarily by confinement degradations associated with 2/1, 3/2, and 1/1 tearing mode activity. These tearing modes had some of the characteristics of neoclassical tearing modes, but often did not seem to require a triggering or seeding event to initiate. Error field seeding and impurities likely contributed to this operational limit.

The NSTX design target [4] which utilizes wall stabilization to achieve $\beta_N = 8.5$ and high $\epsilon\beta_P \approx 1$ to achieve high bootstrap fraction is shown by the star symbol in Figure 3. As seen in the figure, $\epsilon\beta_P$ values

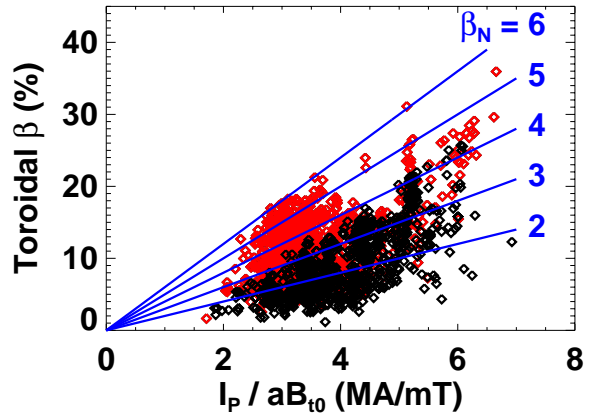


Figure 2: NSTX peak toroidal β values plotted versus normalized current before (black) and after (red) error field reduction and high temperature bake-out.

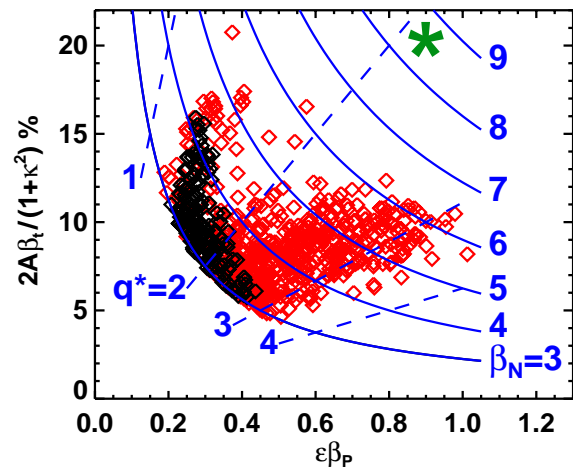


Figure 3: Peak re-scaled toroidal β values plotted versus poloidal beta before (black) and after (red) machine improvements. Only discharges with $\beta_N \geq 3$ are plotted. The NSTX design target is indicated by the star symbol.

in the desired range have now been achieved - but only at cylindrical safety factor $q^* \equiv \epsilon(1 + \kappa^2)\pi a B_{t0}/\mu_0 I_P$ values near 3. To approach the NSTX design target, β_N must increase by roughly 35% at significantly lower $q^* \approx 2$. The design target also has a total pressure peaking factor in the range of 1.8-2 and a monotonic safety factor profile with $q \geq 2$ across the profile. The hollow current density profile consistent with the large off-axis bootstrap current density results in a very low internal inductance $l_i \approx 0.2$ in the target configuration.

4. High β_t disruptions

Neoclassical tearing modes have already been shown to be a concern [12] for any ST operating regime which relies upon high poloidal beta and bootstrap fraction. For operating conditions following machine improvements, Figure 3 shows that the present operating limit of $\beta_N \approx 6$ restricts the accessible β_P and bootstrap fraction for the highest β_t discharges at low $q^* \leq 2$. Such discharges also often have low central safety factor near 1 at high β . In such discharges, large internal $m/n=1/1$ modes can lead to saturation in β , degradation in plasma rotation, and sometimes rapid disruption.

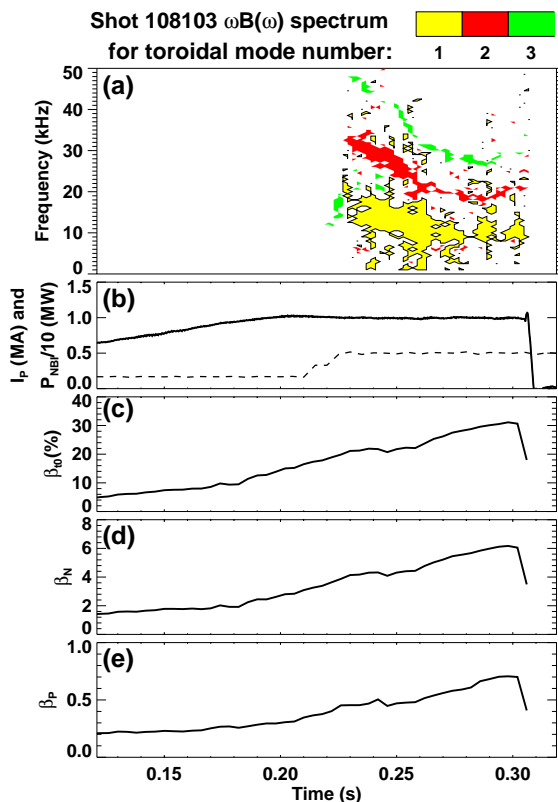


Figure 4: (a) Mirnov spectrogram for toroidal mode numbers $n=1-3$ for the highest $\beta_N=6.2$ discharge (108103) obtained at high toroidal β with $\beta_t=31\%$. Also shown are (b) I_P (solid) and P_{NBI} (dashed), (c) β_t , (d) β_N , and (e) β_P versus time for the same discharge.

An example of such behavior for a 1MA discharge which reaches $\beta_t=31\%$ is shown in Figure 4. As seen in the figure, an $n=1$ mode becomes unstable near $t=220$ ms following $q(0)$ reaching 1 near $t=200$ ms (not shown). As seen in Figures 4c-e, the various β parameters exhibit saturation from $t=225-260$ ms despite the previous increase in NBI heating power by a factor of 3. Most discharges in this parameter range never recover from the onset of this mode and exhibit beta limits of $\beta_P \approx 0.5$ and $\beta_N \approx 4-4.5$. The discharge in Figure 4 is unique in that the limiting mode amplitude decreases after $t=260$ ms allowing the β to increase and ultimately reach $\beta_P \approx 0.7$ and $\beta_N \approx 6.2$ prior to undergoing an uncommonly rapid 400MA/s plasma current disruption.

Insight into the structure of this β -limiting 1/1 mode can be gained from correlating the plasma rotation profiles to fluctuation spectra from the NSTX ultra-soft X-ray (USXR) array [13]. Figure 5 shows that the chords with highest emission fluctuation amplitude correlate well in both frequency and minor radius with regions of flattened angular frequency measured using carbon charge exchange recombination spectroscopy [14].

This figure also indicates that the mode initiates in the core far from the 2/1 surface but inside the $q=1$ surface. Later in time at $t=280\text{ms}$, the mode radius has grown to $r/a = 0.4-0.5$, and the localization of the rotation flattening likely indicates the presence of a large 1/1 island. Near $t=305\text{ms}$, the mode grows further, slows, and then locks leading to discharge termination. From the discussion above, it is evident that highest β_t discharges in NSTX can clearly be limited in performance by tearing modes. However, the role of neoclassical drive in the mode growth is not yet clear, as many such discharges operate near the beta limit for internal pressure driven kink modes. In particular, the classical tearing drive can be naturally strong due to positive tearing index Δ' [15] computed near ideal limits.

5. High β_P disruptions

Figure 6 plots the time dependence of several parameters of an $I_P = 800\text{kA}$, $B_{t0}=5\text{kG}$, $P_{NBI}=6\text{MW}$ lower single null H-mode discharge which reaches $\beta_t=17\%$ and $\beta_P = 1.4$. As seen in Figures 6a-c, $q(0)$ and l_i reach quasi-steady values, while the normalized β increases slowly in the 200ms prior to the partial collapses and eventual disruption in plasma stored energy. Figure 6d shows that the total pressure peaking factors from EFIT (solid line) and TRANSP [16] (dotted line) also reach nearly constant values. In this figure, the EFIT pressure profile is loosely constrained by the shape of the electron pressure profile. However, this discharge does not achieve density flat-top, and the fraction of stored energy in the fast ion component is decreasing as a function of time. The thermal pressure profile (shown by the dashed line in Figure 6d) is found to increase in peaking factor as the H-mode density profile transitions from hollow to monotonic. Thus the total pressure profile shape is changing in this discharge while keeping the peaking factor nearly constant. Finally, Figure 6e shows that there is a small 0.5 Gauss precursor roughly 30ms prior to the final collapse of the discharge. Details of RWM signatures, toroidal flow damping, and critical rotation threshold physics in these and similar collapses are discussed in more detail in Reference [17].

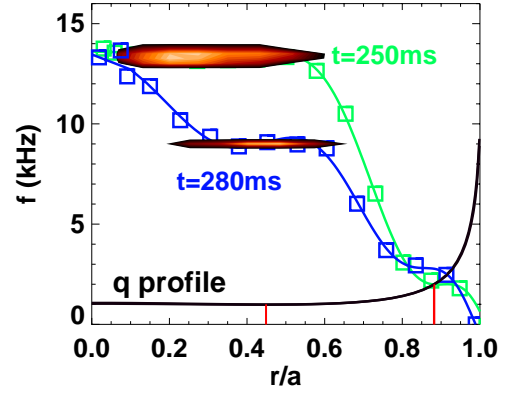


Figure 5: Carbon impurity rotation profiles and USXR frequency spectra (overlaid) versus minor radius at $t=250$ and 280ms prior to disruption of the discharge shown in Figure 4.

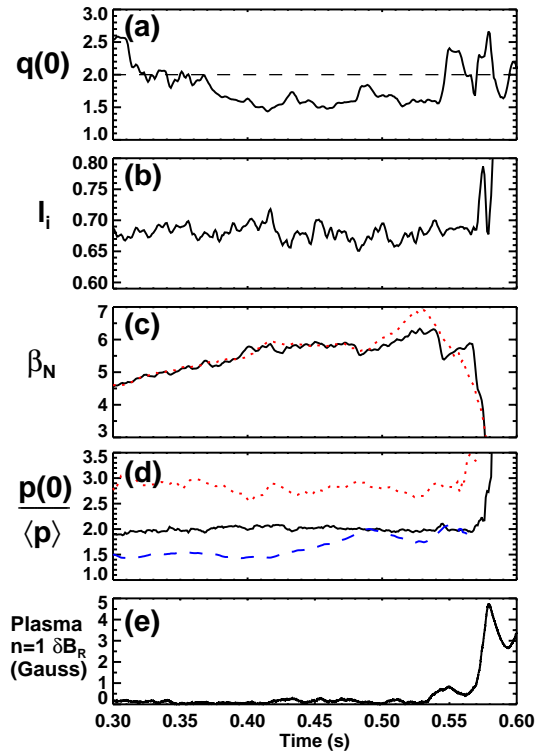


Figure 6: Time traces of (a) central safety factor, (b) internal inductance, (c) normalized beta, (d) pressure peaking factor, and (e) locked mode signal for high β_N shot 109070. Solid lines indicate results from EFIT and dotted lines correspond to TRANSP results. Dashed line in (d) corresponds to thermal pressure peaking.

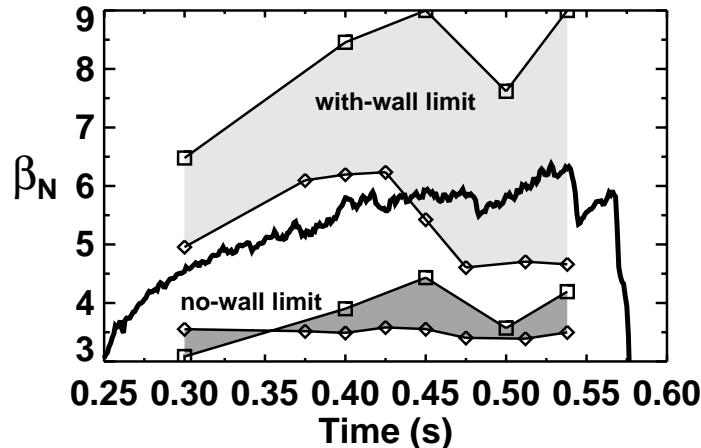


Figure 7: $n=1$ kink mode no-wall (lower shaded region) and with-wall (upper shaded region) marginally stable β_N for the discharge of Figure 6. Square symbols correspond to marginal β_N values for the EFIT pressure profile, diamonds to the TRANSP pressure profile.

Figure 7 shows the computed no-wall and with-wall β_N limits as a function of time preceding the collapse in stored energy for both the EFIT and TRANSP pressure profiles for shot 109070. In these calculations, the EFIT and TRANSP equilibrium solutions are refined with the J-SOLVER [18] flux coordinate equilibrium solver, and the q profile is approximately fixed to be that from partial-kinetic EFIT by choosing a parallel current density profile consistent with the pressure profile at the equilibrium β value. The equilibrium boundary is chosen to be at the surface where 99-99.5% of the poloidal flux is enclosed, and the edge safety factor value is chosen to be just above an integer value to eliminate surface kink modes which might otherwise result from the necessary elimination of the separatrix in the fixed boundary stability calculations using DCON [19]. As seen in the figure, the discharge is computed to exceed the no-wall β_N limit = 3-4 independent of which pressure profile is assumed. However, the predicted with-wall limit is found to be more sensitive to variations in the pressure profile peaking, and the experimental β_N value is found to cross the with-wall stability limit near $t=450$ ms using the TRANSP pressure profile, but to not reach this limit if the broader EFIT profile is used. However, both limits exhibit a decrease in the marginal β_N after $t \approx 450$ ms, so a decreasing with-wall β limit due to an evolving pressure (and possibly current) profile combined with a slowly increasing β may together explain the disruptions near the end of the discharge.

6. Effects of rapid rotation

The high rotation speed of many NSTX discharges not only impacts β limits through wall stabilization, but can also modify the underlying equilibrium itself. As mentioned previously, rotation speeds as high as 0.2 times the local Alfvén speed are not uncommon in the core of NSTX plasmas, and in diamagnetic discharges the rotational Alfvén Mach number $M_A \equiv v_\phi/v_A$ can be as high as 0.3. The centrifugal force of the spinning plasma most strongly modifies force balance near the magnetic axis, where the pressure gradient would otherwise be small. Assuming the thermal temperatures are poloidal flux functions, the shift of peak pressure outward from the magnetic axis should imply an even larger increase in the major radius of maximum density and finite density gradient at the axis.

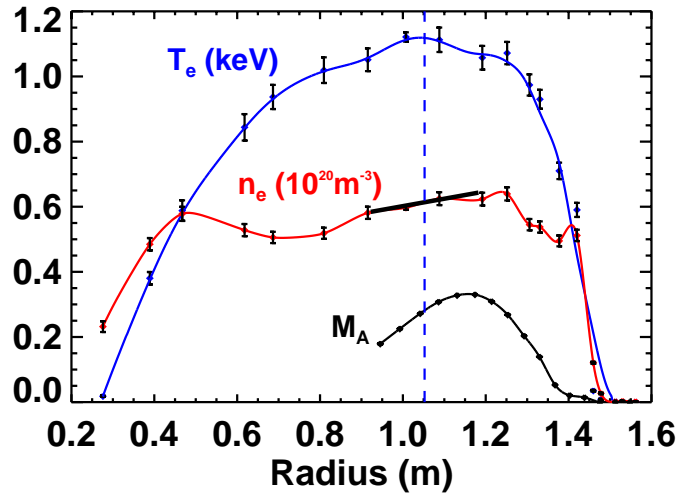


Figure 8: Profiles of electron temperature, electron density, and rotational Alfvén Mach number plotted versus major radius for shot 109070 at $t=530$ ms.

This shift in density is indeed observable as seen in Figure 8 which plots profiles of electron temperature, electron density, and M_A for discharge 109070 at $t=530$ ms. At this time, the plasma has become slightly diamagnetic and M_A at the magnetic axis indicated by the vertical dashed line reaches 0.25. At the axis, radial force balance dictates that $R(d[\log(n_e)]/dR) = 2M_A^2/\beta_{local}$. The solid line overlaying the density profile in the figure indicates the gradient expected from this force balance equation and is in good agreement with the measured core gradient. The centrifugal force of the fast ion component must in general be included in the core force balance, but for the high density plasmas treated here, the thermal component is dominant.

Finally, in addition to strong flow modifying equilibria, flow shear may also impact MHD stability. Initial calculations using the M3D code for NSTX [20] find that for self-consistent MHD equilibria with flow included, linear growth rates of $n=1$ internal pressure-driven kink modes with $q(0) < 1$ can be reduced by as much as a factor of 3 due to flow shear. Fast particle effects, two-fluid effects, and having $q(0) > 1$ are all further stabilizing, and non-linearly saturated states with β values significantly above ideal-marginal values appear possible. Determining if such effects are contributing to the achievement of very high β values for plasmas like that shown in Figure 4 is a topic for future research.

7. Summary

Device and operational improvements have led to a significant increase in global magnetohydrodynamic stability limits in NSTX plasmas. Pressure profile broadening from H-mode operation combined with reduced error fields now allow access to normalized beta values as high as $\beta_N = 6.5$ and $\langle\beta_N\rangle = 4.5$. Maximum toroidal beta values have reached $\beta_t = 35\%$ and volume-average beta values $\langle\beta\rangle=15\%$. High poloidal beta operation with $\beta_P \leq 1.4$ has allowed a doubling of discharge pulse-length to just over 1 second with sustained periods of $\beta_N \approx 6$. High β_N values have been achieved at low internal inductance with $\beta_N/l_i \leq 10$. Stability analysis indicates that many of the high β_P discharges at high β_N are routinely operating above the no-wall stability limit and may be disrupting at

least in part due to proximity to the with-wall limit. Central rotation damping is often observed to precede thermal disruption in these discharges and may be evidence for the destabilization of resistive wall modes. Long-lived 2/1 or 3/1 tearing modes are also observed at large minor radius in these discharges, and these modes appear to impact edge confinement without significantly degrading the overall discharge. At higher β_t and lower q , core 1/1 modes are found to most often saturate β and β_P , although very rapid current and thermal disruption is sometimes observed. Rapid rotation from unidirectional beam injection is observed to modify radial force balance such that pressure and density are no longer flux functions. In addition, large rotational shear has been theoretically shown to help suppress internal kink modes and may contribute to the saturation of 1/1 modes in the highest β_t discharges of NSTX.

Acknowledgments

This work was supported by the United States Department of Energy under contract numbers DE-AC02-76CH03037 (PPPL), DE-AC05-00R22725 (ORNL), W-7405-ENG-36 (LANL) and grant numbers DE-FG02-99ER54524 (CU), DE-FG02-99ER54523 (JHU).

References

- [1] ONO, M., et al., Nucl. Fus. **40** (2000) 557.
- [2] KAYE, S., et al., Fus. Technol. **36** (1999) 16.
- [3] MAINGI, et al., Paper EX/C2-5 this conference.
- [4] MENARD, J. E., et al., Nucl. Fus. **37** (1997) 595.
- [5] PAOLETTI, F., et al., Nucl. Fus. **42** (2002) 418.
- [6] MAINGI, R., et al., Phys. Rev. Lett. **88** (2002) 035003.
- [7] LAO, L. L., et al., Nucl. Fus. **25** (1985) 1611.
- [8] SABBAGH, S. A., et al., Nucl. Fus. **41** (2001) 1601.
- [9] SABBAGH, S. A., et al., Phys. Plasmas **9** (2002) 2085.
- [10] SYKES, A., et al., *Proceedings of the 11th European Conference on Controlled Fusion and Plasma Physics, Aachen, Germany, 1983*, volume 7D, Part II, p. 363, Switzerland, 1983, European Physical Society, Petit-Lancy.
- [11] TROYON, F., et al., Plasma Phys. and Contr. Fus. **26** (1984) 209.
- [12] BUTTERY, R. J., et al., Phys. Rev. Lett. **88** (2002) 125005.
- [13] STUTMAN, D., et al., Rev. Sci. Instrum. **70** (1999) 572.
- [14] BELL, R., et al., Technical Report 3591, PPPL, 2001.
- [15] BRENNAN, D. P., et al., Phys. Plasmas **9** (2002) 2998.
- [16] GOLDSTON, R. J., et al., J. Comput. Phys. **43** (1981) 61.
- [17] SABBAGH, S., et al., Paper EX/S2-2 this conference.
- [18] DELUCIA, J., et al., J. Comput. Phys. **37** (1980) 183.
- [19] GLASSER, A. and CHANCE, M., Bull. Am. Phys. Soc. **42** (1997) 1848.
- [20] PARK, W., et al., Paper TH/5-1 this conference.